

NATIONAL AERONAUTICS AND SPACE ADMINISTRATION

*Technical Report 32-1307*

*Consistency of Lunar Orbiter Residuals  
With Trajectory and Local  
Gravity Effects*

*Paul M. Muller  
William L. Sjogren*

GPO PRICE \$ \_\_\_\_\_

CSFTI PRICE(S) \$ \_\_\_\_\_

Hard copy (HC) \_\_\_\_\_

Microfiche (MF) \_\_\_\_\_

ff 653 July 65

**N 68-34045**

FACILITY FORM 602

(ACCESSION NUMBER) \_\_\_\_\_ (THRU) \_\_\_\_\_

28 (PAGES) \_\_\_\_\_ (CODE) \_\_\_\_\_

CR-96735 (NASA CR OR TMX OR AD NUMBER) \_\_\_\_\_ (CATEGORY) 30

JET PROPULSION LABORATORY  
CALIFORNIA INSTITUTE OF TECHNOLOGY  
PASADENA, CALIFORNIA

September 1, 1968



NATIONAL AERONAUTICS AND SPACE ADMINISTRATION

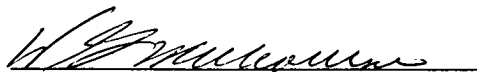
*Technical Report 32-1307*

*Consistency of Lunar Orbiter Residuals  
With Trajectory and Local  
Gravity Effects*

*Paul M. Muller*

*William L. Sjogren*

Approved by:



W. G. Melbourne, Manager  
Systems Analysis Research Section

JET PROPULSION LABORATORY  
CALIFORNIA INSTITUTE OF TECHNOLOGY  
PASADENA, CALIFORNIA

September 1, 1968

**TECHNICAL REPORT 32-1307**

Copyright © 1968  
Jet Propulsion Laboratory  
California Institute of Technology

Prepared Under Contract No. NAS 7-100  
National Aeronautics & Space Administration

## Contents

<b>I. Introduction</b> . . . . .	1
<b>II. Method of Attack</b> . . . . .	2
<b>III. Background</b> . . . . .	2
<b>IV. Results</b> . . . . .	2
<b>V. Additional Cases and Evaluation of the SPODP and Polynomial Models</b> . . . . .	13
<b>VI. Possible Direction of Future Work</b> . . . . .	19
<b>VII. Summary</b> . . . . .	20
<b>Appendix A.</b> The Polynomial Fitting Program and Method . . . . .	21
<b>Appendix B.</b> Polynomial Model Coefficients Nomenclature . . . . .	22
<b>References</b> . . . . .	22
<b>Tables</b>	
1. Lunar harmonic coefficient sets . . . . .	7
2. Probe conditions in selenocentric cartesian coordinates . . . . .	9
<b>Figures</b>	
1. Plot of lunar tracks for trajectories studied . . . . .	3
2. ODP fit to one orbit of <i>Lunar Orbiter III-E, 3</i> with three lunar potential models . . . . .	4
3. Integrated trajectory residuals . . . . .	5
4. Lunar contours . . . . .	6
5. Relative harmonic spectrum of <i>Lunar Orbiter III-E, 3</i> . . . . .	6
6. Polynomial fits to four distinct orbits of <i>Lunar Orbiter III-E, 1</i> and 2 . . . . .	8
7. Comparison of ODP and polynomial fits to two distinct orbits of <i>Lunar Orbiter III-E, 1</i> . . . . .	10
8. Polynomial fits to three distinct orbits of <i>Lunar Orbiter III-E, 3</i> and 4 with one ODP fit for comparison . . . . .	11
9. Comparison of ODP fits to two distinct spacecraft ( <i>Lunar Orbiters IV-C</i> and <i>V-C</i> ) with similar trajectories . . . . .	12

## Contents (contd)

### Figures (contd)

10. ODP fits to one orbit of <i>Lunar Orbiter III-E</i> , 3 with distinct epoch and fit lengths . . . . .	13
11. Polynomial fits to one orbit of <i>Lunar Orbiter III-E</i> , 2 with distinct epochs and coefficient sets . . . . .	14
12. Comparison of residuals from <i>Lunar Orbiter I-B</i> , 3 in region of pericenter passage as determined by three distinct methods of computation . . . . .	15
13. Polynomial fits to one orbit of <i>Lunar Orbiter I-B</i> , 3 and to central 80 min, only, with two coefficient sets . . . . .	16
14. ODP fits to two distinct spacecraft in three orbits, <i>Lunar Orbiters I-B</i> , 1; <i>I-B</i> , 3; and <i>II-B</i> . . . . .	17
15. Polynomial fits to two distinct spacecraft orbits, <i>Lunar Orbiters I-B</i> and <i>II-B</i> . . . . .	18

## Abstract

The fits to earth-based coherent two-way radio doppler data from the *Lunar Orbiters* have consistently yielded residuals three orders of magnitude larger than the 0.1 mm/s normally observed with spacecraft at lunar distance. An intensive analysis of this problem has demonstrated a 1:1 correlation between residuals and position on the lunar track which eliminates other forces, and ties the residuals to local lunar gravity effects. The possibility that software was inducing the variations was eliminated by duplicating the residuals with a polynomial fit to the raw data. The results suggest need for a new or modified approach to the lunar potential model that would include one or more of the following characteristics: (1) higher order spherical harmonics, (2) point mass grid solutions, (3) direct mapping of residual-accelerations to the lunar surface.

# Consistency of Lunar Orbiter Residuals with Trajectory and Local Gravity Effects

## I. Introduction

This report describes one phase of the effort devoted to analyzing the doppler tracking data from the five NASA *Lunar Orbiter* missions. The total effort has two primary goals: (1) to obtain a description of the moon's gravity field for scientific interest and application and (2) to obtain a representation of the moon's gravity field that is adequate for *Apollo* operations.

To date, the scientific analysis has proceeded with the immediate objective of determining the zonal and low-degree tesseral harmonics that describe the large-scale variations from sphericity; however, for *Apollo* application, since precise short-term prediction of spacecraft position is a requirement, more localized effects appear to be important. Apparently, the low-degree harmonics are not adequate for this purpose.

A more intense study of the short-period fluctuations in the doppler data was initiated. Throughout the *Lunar Orbiter* program, it had been noticed that the doppler data exhibited short-period variations that could not be

accounted for by any moon-model then available. This characteristic suggested that either (1) the doppler data were in error or (2) data were being analyzed incorrectly or (3) the moon was rougher than anticipated. By a process of elimination, Lorell and Sjogren (Ref. 1) concluded that the gravitational roughness was the most likely cause.

Short-period effects suggest correlation either with surface features of the moon or, at least, with positions on the lunar surface. Early attempts to find such correlations were unsuccessful. However, a breakthrough in this direction was effected with the discovery that, when doppler residuals from single-orbit data fits were examined, the resulting residuals correlated closely with spacecraft position above the moon and were consistent from orbit to orbit. Two factors were necessary for this correlation: (1) the use of only one orbit of data in the orbit determination and (2) the use of a simple harmonic model of the moon—e.g., spherical or triaxial. This report describes a study of the correlation phenomenon, and the possible implications with respect both to *Apollo* applications and to general scientific applications.

## II. Method of Attack

There are three basic sources for residuals after the fit to a spacecraft trajectory:

1. From such forces as gravity, solar pressure, gas jets, and others that act on the spacecraft directly
2. From errors and physical deformations that affect the data tracking system—e.g., temperature couples to the transponder and tropospheric refraction
3. From software problems wherein the computer programs introduce residuals because of model limitations or program errors

In short, the sources are physical forces, data tracking errors, and software.

Sources in the software category would be eliminated by producing the same residuals with an independent program such as a polynomial fit to the raw tracking data. Except for lunar gravity,<sup>1</sup> effects associated with the first two categories cited above would be eliminated if the same *and* distinct spacecraft produced the same residuals when flying similar trajectories. The reported study was based on these fundamental principles. As noted in the introduction, fits to single orbits with a simplified potential model were used for the comparisons.

## III. Background

The authors were inclined to believe the basic hypothesis that the tracking data residuals can be correlated with the spacecraft lunar track,<sup>2</sup> in view of the results obtained from a simple calculation relating spacecraft accelerations (as determined from the residuals) to the accelerations that could reasonably be expected from the variations in lunar terrain.

Examination of residuals such as those in Fig. 2 shows common variations of 0.5 Hz in a period of 5 min, which corresponds to an acceleration  $a$  of 0.1 mm/s<sup>2</sup>. This is equivalent to a perturbing mass equal to one-millionth of the lunar mass at a distance of 190 km (i.e.,  $m_{\text{perturb}} = ar^2$ ). This amount of mass-differential is contained in a  $100 \times 100 \times 2$ -km depression for a lunar density of 3.3.

<sup>1</sup>Relationship between gravity-gradient forces on the spacecraft with gas-jet reactions were eliminated in Ref. 1 for reasons of insufficient amplitude.

<sup>2</sup>By "lunar track" is meant the track on the lunar surface formed by the intersection of the spacecraft orbit plane with the lunar surface. Figure 1 shows lunar tracks of various orbits of the *Lunar Orbiters*.

These numbers are in good agreement with the observed condition of the lunar surface. If the local irregularities are large enough to cause the perturbations, perhaps they, also, are responsible.

Figure 3 shows the variations caused by a set of alternating mass points that are one-millionth of the lunar mass, spaced equally in time on the lunar surface directly below a spacecraft trajectory (*Lunar Orbiter III*, phase E). The residual plot was produced by differencing the doppler obtained from a spherical moon trajectory (unperturbed) and the perturbed trajectory resulting from the added mass points.

Figure 2 indicates another clue to the applicable method. A glance at the plot shows that the residual frequencies range between 5 and 15 cycles per spacecraft orbit, which is far too high to be handled by the current comparatively low-order harmonic models for the moon. Figure 2 defines the single precision orbit determination program [SPODP (Ref. 2)] fits to the same data by use of triaxial, COSPAR, and JPL No. 87 harmonic sets. (The model-coefficients are listed in Table 1.) The first model is clearly superior for short arcs and, therefore, was used in this study, as noted above. The larger harmonic models were intended to fit the longer arcs, and they are applied well in that context.

Figure 4 also demonstrates the relative coarseness of current harmonic models. The first part of the figure was obtained by setting  $C_{44} = 10^{-6}$  (a typical size), with the remaining coefficients all *zero*, and plotting the relative elevations that would match this single harmonic, the highest order term in the JPL model. Figure 4b is a plot, as above, from the COSPAR harmonic set as listed in Table 1. Apparently, the resulting surfaces are too smooth to account for the observed residual frequencies.

Additional confirmation of the residual frequencies is contained in Fig. 5, which is a harmonic spectrum of the residuals plotted in Fig. 2. There is a lack of low-order frequency because of the short data span; however, the plot is representative of the highest frequency residuals observed and indicates rather strongly that low-order harmonic expansions of the lunar field will not improve the short arc fits.

## IV. Results

Before comparison of the residuals could be accomplished with confidence, it had first to be shown that the SPODP (Ref. 2) could produce consistent solutions.



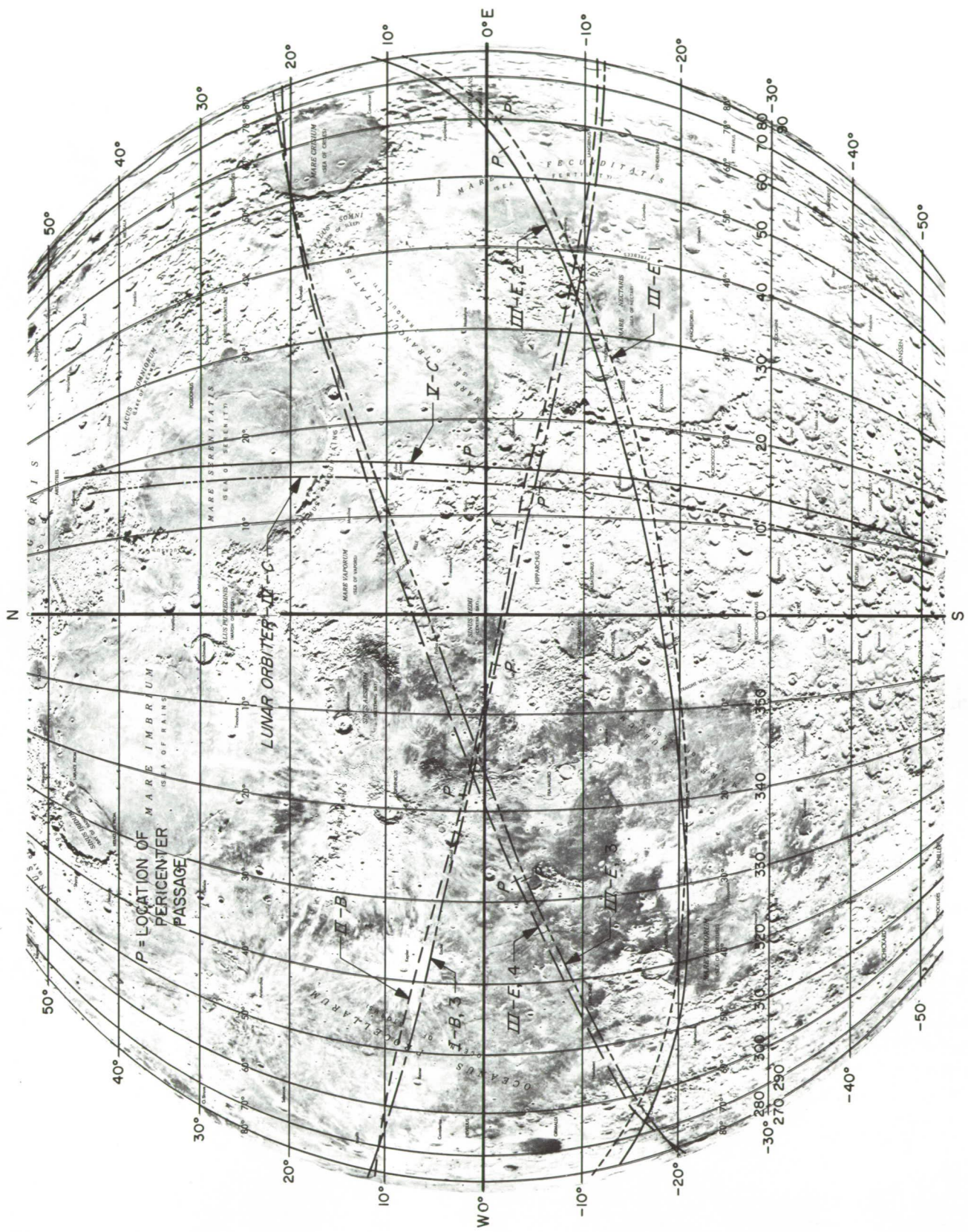


Fig. 1. Plot of lunar tracks for trajectories studied

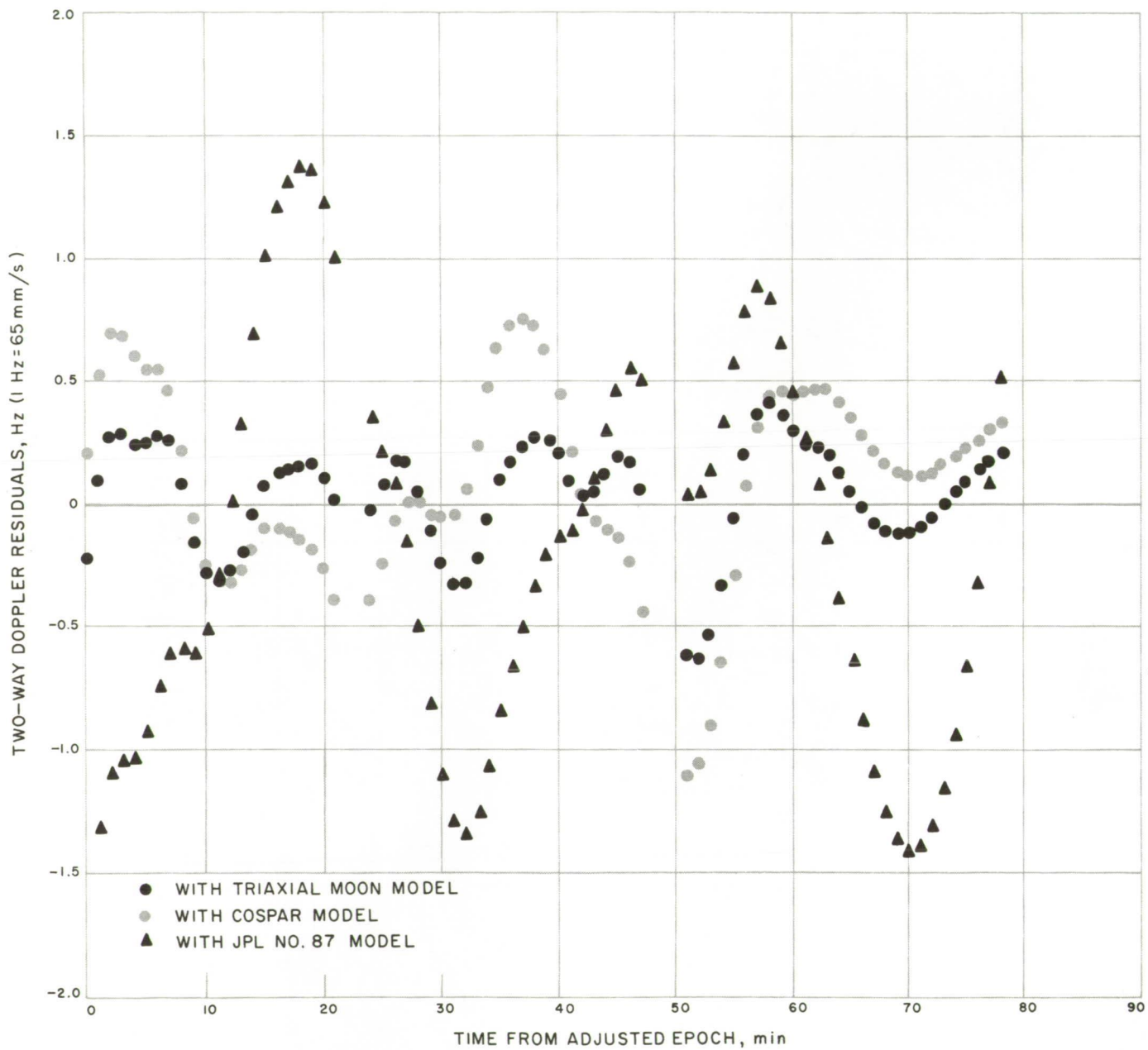


Fig. 2. ODP fit to one orbit of *Lunar Orbiter III-E, 3* with three lunar potential models

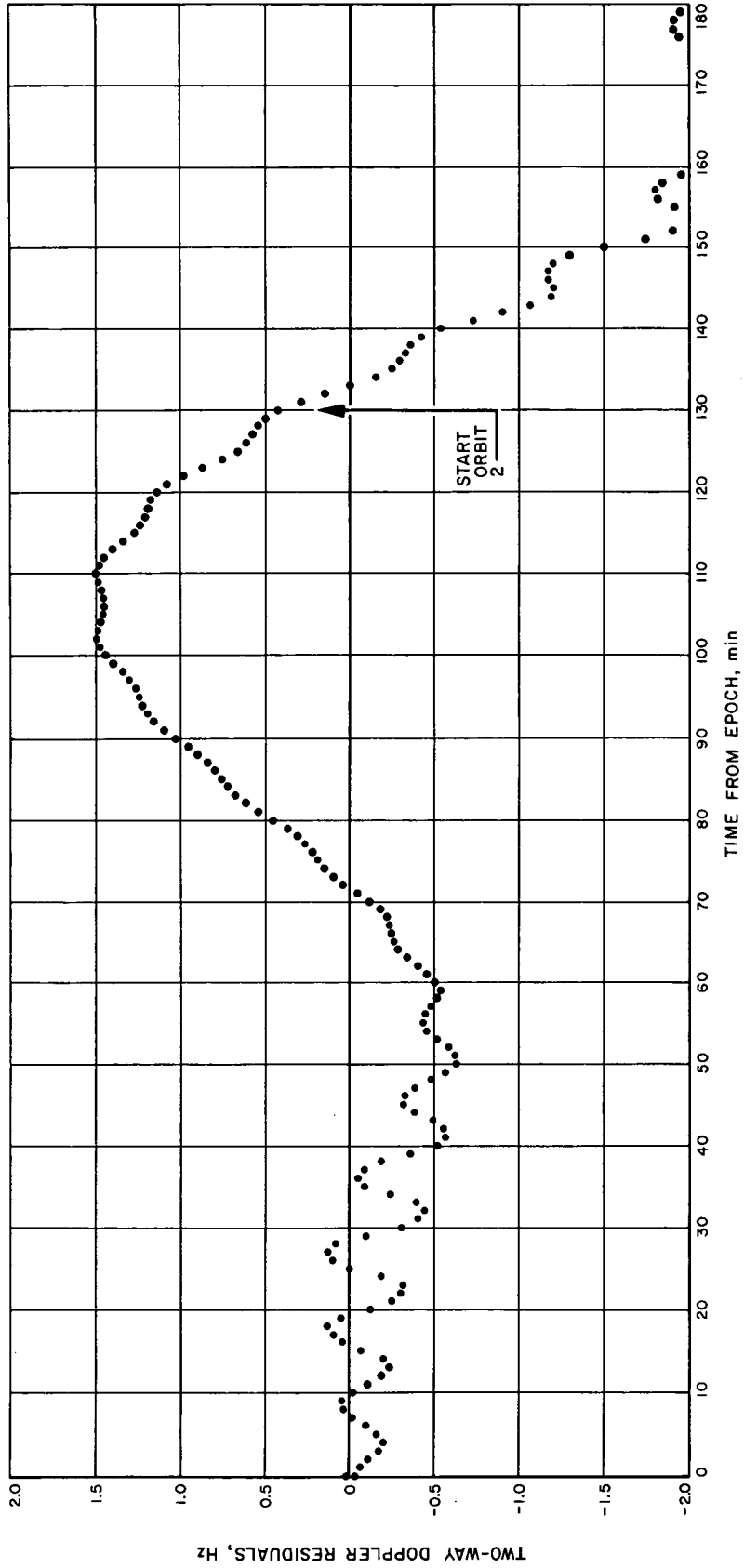


Fig. 3. Integrated trajectory residuals

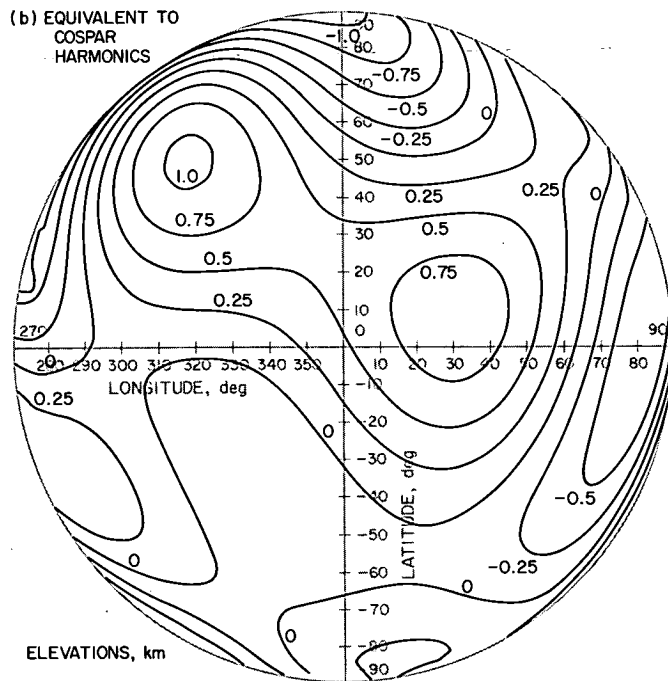
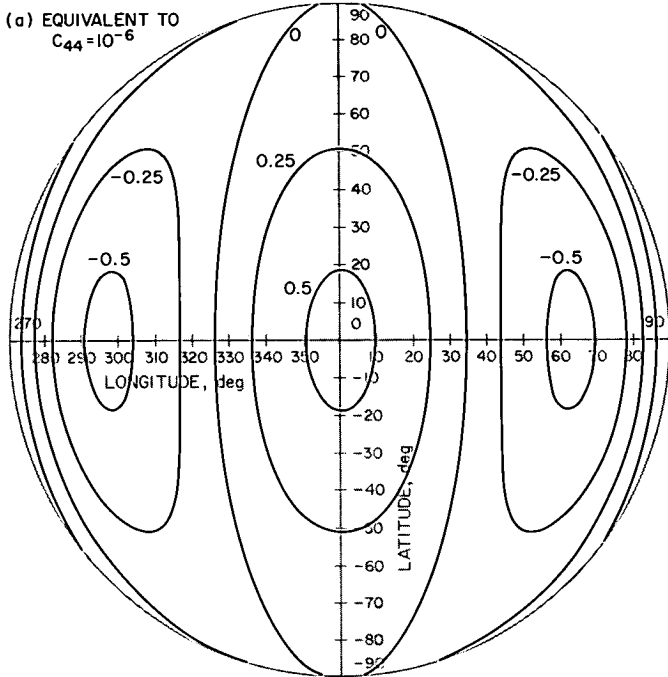


Fig. 4. Lunar contours

Earlier attempts to compare residuals (using 2-orbit fits) were not successful because the SPODP will not consistently fit the same data region unless the data span is one orbit or less. Currently, study is being made of the SPODP limitations for longer arcs; the results of that

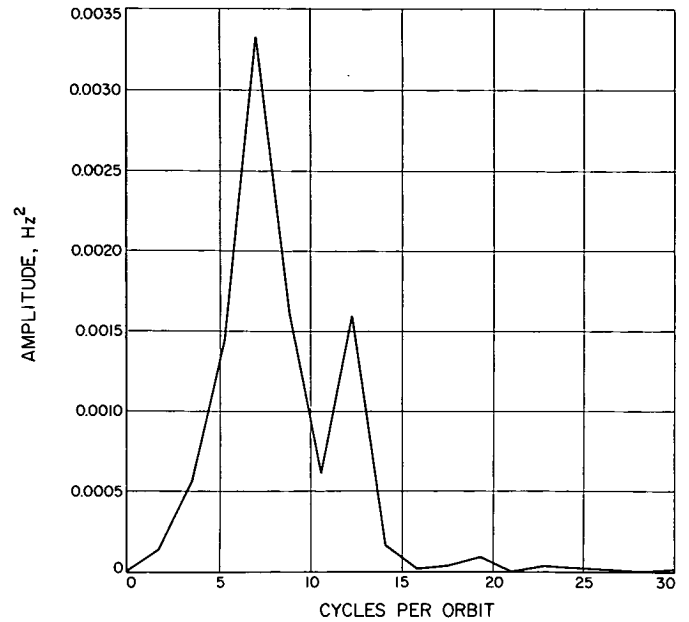


Fig. 5. Relative harmonic spectrum of Lunar Orbiter III-E, 3 1-orbit residuals

work, which are beyond the scope of this paper, will be reported later.

To demonstrate consistency, short *Apollo* type (*Lunar Orbiter III-E*, eccentricity  $\approx 0$ ) arcs were fit with different epochs and lengths of data span. Results are shown in Fig. 6. (Table 2 lists orbital characteristics for all trajectories.) This agreement gave confidence in comparisons between trajectories, providing the outlined fitting policy was followed.

For the independent software, a new program and system, devised by Peter Dyer and Steven McReynolds of JPL, was employed. The program fits a polynomial directly to the raw doppler data and removes the station motion with a second-degree polynomial; and the spacecraft motion is removed with a second-order elliptical function based on the period of the orbit involved.<sup>3</sup>

The residuals shown in Figs. 7 and 8, which compare the sample trajectories, have been plotted with respect to an adjusted time parameter. In each case, the epoch has been altered to be a point at which the two trajectories are most nearly above the same lunar location;

<sup>3</sup>A number of earlier attempts to fit the raw doppler here at JPL had failed, and success of this particular system is considered by the authors to have been a significant breakthrough.

Table 1. Lunar harmonic coefficient sets

Nominal triaxial set					
Harmonic	Coefficient	Harmonic	Coefficient	Harmonic	Coefficient
$J_{20}$	$0.2073 \times 10^{-3}$	$C_{22}$	$0.2030 \times 10^{-4}$		
COSPAR set <sup>a</sup>					
$J_{20}$	$0.2059 \times 10^{-3}$	$C_{22}$	$0.2042 \times 10^{-4}$	$S_{21}$	$0.8 \times 10^{-6}$
$J_{30}$	$0.3373 \times 10^{-4}$	$C_{32}$	$0.1294 \times 10^{-4}$	$S_{22}$	$-0.342 \times 10^{-5}$
$J_{40}$	$-0.798 \times 10^{-5}$	$C_{33}$	$0.317 \times 10^{-5}$	$S_{31}$	$0.1762 \times 10^{-4}$
$J_{50}$	$0.5505 \times 10^{-4}$	$C_{42}$	$0.11 \times 10^{-6}$	$S_{32}$	$-0.147 \times 10^{-5}$
		$C_{43}$	$-0.82 \times 10^{-6}$	$S_{33}$	$-0.43 \times 10^{-6}$
		$C_{44}$	$-0.070 \times 10^{-7}$	$S_{41}$	$0.391 \times 10^{-5}$
		$C_{51}$	$-0.385 \times 10^{-5}$	$S_{42}$	$0.72 \times 10^{-6}$
		$C_{52}$	$0.342 \times 10^{-5}$	$S_{43}$	$-0.1 \times 10^{-7}$
		$C_{53}$	$-0.71 \times 10^{-6}$	$S_{44}$	$0.11 \times 10^{-6}$
		$C_{54}$	$-0.8 \times 10^{-7}$	$S_{51}$	$0.829 \times 10^{-5}$
		$C_{55}$	$-0.3 \times 10^{-7}$	$S_{52}$	$-0.203 \times 10^{-5}$
				$S_{53}$	$-0.78 \times 10^{-6}$
				$S_{54}$	$-0.13 \times 10^{-6}$
				$S_{55}$	$0.3 \times 10^{-7}$
JPL No. 87 set <sup>b</sup>					
$J_{20}$	$0.190 \times 10^{-3}$	$C_{21}$	$0.258 \times 10^{-5}$	$S_{21}$	$0.273 \times 10^{-5}$
$J_{30}$	$0.204 \times 10^{-4}$	$C_{22}$	$0.896 \times 10^{-5}$	$S_{22}$	$-0.108 \times 10^{-4}$
$J_{40}$	$-0.131 \times 10^{-4}$	$C_{31}$	$0.339 \times 10^{-4}$	$S_{31}$	$0.104 \times 10^{-4}$
$J_{50}$	$-0.202 \times 10^{-5}$	$C_{32}$	$-0.402 \times 10^{-6}$	$S_{32}$	$0.304 \times 10^{-5}$
$J_{60}$	$0.137 \times 10^{-4}$	$C_{33}$	$0.411 \times 10^{-5}$	$S_{33}$	$-0.309 \times 10^{-5}$
$J_{70}$	$-0.400 \times 10^{-4}$	$C_{41}$	$-0.109 \times 10^{-4}$	$S_{41}$	$0.787 \times 10^{-5}$
$J_{80}$	$0.206 \times 10^{-4}$	$C_{42}$	$0.420 \times 10^{-5}$	$S_{42}$	$0.525 \times 10^{-6}$
		$C_{43}$	$0.232 \times 10^{-5}$	$S_{43}$	$-0.102 \times 10^{-5}$
		$C_{44}$	$-0.588 \times 10^{-6}$	$S_{44}$	$-0.201 \times 10^{-6}$

<sup>a</sup>Adopted by IV IQSY/COSPAR Assembly and Joint IQSY-COSPAR Symposium, July 17-22, 1967, London (Ref. 3).

<sup>b</sup>An interim set of coefficients supplied by Jack Lorell of JPL, not necessarily definitive.

this was done to show the residual agreement as a function of the lunar track. It was discovered that the epoch-difference could be derived either by consulting the trajectory listings from SPODP or by simply overlaying the original plots and reading the time difference. The agreement of residuals for the sample trajectories confirmed the contention that the residuals are tied to the lunar surface.

Figure 7, by itself, covers the kernel of the study. Figure 7a shows a fit to an *Apollo* (low eccentricity) type orbit, *Lunar Orbiter III-E*, data package 1 (an arbitrary JPL numbering system to identify the data ranges). Figure 7b is an SPODP fit to the spacecraft data just two orbits later. In this time, the trajectories have changed considerably less than the perilune distance of 150 km

and are, therefore, essentially identical as far as the perturbations are concerned.

Figure 7c is a *polynomial* fit to the same data as used in part b of that figure. The agreement rules out both the independent software system and the SPODP as a possible causes of the residuals. The independent software check builds confidence that SPODP is yielding the true residuals.<sup>4</sup>

<sup>4</sup>By "true" residuals we mean those directly attributable to, and correlated with, the lunar track and invariant under changes to the fit-epoch and data span within the guidelines of one orbit maximum and basic harmonics. The polynomial fits show both that the software is correct and that the observed residuals are true in the above sense. Reference 1 obtained favorable comparison between the JPL and Langley programs for two orbit fits and, thereby, had previously eliminated gross program failure as the cause.

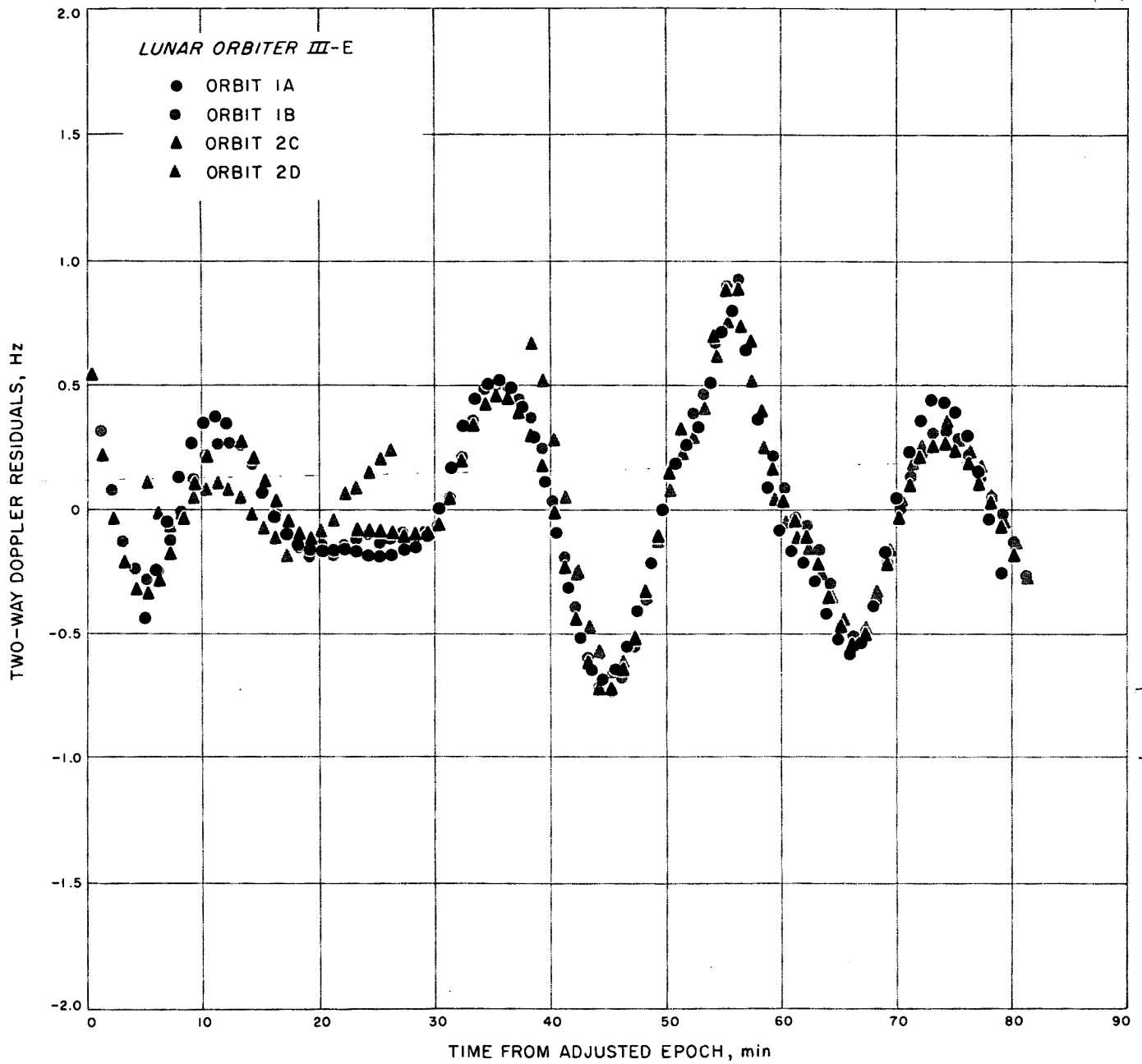


Fig. 6. Polynomial fits to four distinct orbits of *Lunar Orbiter III-E*, 1 and 2

Table 2. Probe conditions in selenocentric cartesian coordinates

Source	Orbit of Lunar Orbiter (model and phase), number in series										
	III-E, 1a <sup>a</sup>	III-E, 2c <sup>a</sup>	III-E, 3	III-E, 4a <sup>a</sup>	I-B, 1	I-B, 3	II-B	IV-C	V-C		
x <sup>b</sup> , km	-2038.527	-679.617	1864.971	-435.091	2327.34	2055.469	2435.14	-5518.539	-588.6738		
y <sup>b</sup> , km	222.756	1440.35	-32.9292	-1363.37	-346.9167	-2306.28	1513.20	1166.0388	-1184.352		
z <sup>b</sup> , km	-48.4853	1238.26	262.0641	-1310.581	451.3395	-367.888	1080.60	107.51312	-2648.3518		
Dx <sup>b</sup> , km/s	-0.080334	-1.4600	-0.092526	1.563907	-0.371742	0.562086	-0.96697	0.12103467	0.39887229		
Dy <sup>b</sup> , km/s	-1.107033	-0.25185	1.222368	-0.334627	1.388035	0.879622	0.5591078	0.17154097	1.0701989		
Dz <sup>b</sup> , km/s	-1.02804	-0.41808	1.101003	-0.058935	0.4370867	0.4750692	0.360331	-0.622698	-0.2735364		
Epoch, date and GMT	30 Aug. 67 20:55:00.	31 Aug. 67 00:50:00.	5 Sep. 67 15:05:00.	5 Sep. 67 18:50:00.	25 Aug. 66 16:02:00.	26 Aug. 66 05:19:00.	23 Nov. 66 05:45:00.	13 Jun. 67 20:28:00.	13 Aug. 67 10:05:00.		
Latitude, <sup>c</sup> deg	-2.805	1.772	7.01308	-20.96	12.0989	9.2030	7.0447	-2.6106	-42.4594		
Longitude, <sup>c</sup> deg	251.132	184.7	2.6391	254.28	270.72	219.34	210.667	192.925	199.9674		
Pericenter altitude, km	143.6	144.0	132.0	132.38	40.02	40.639	44.0	68.3	96.1		
Epoch of pericenter passage	30 Aug. 67 21:54:37.3	31 Aug. 67 02:15:54.3	5 Sep. 67 17:05:16.	5 Sep. 67 19:15:46.3	25 Aug. 67 16:32:53.8	26 Aug. 66 06:18:05.6	23 Nov. 66 06:40:59.9	13 Jun. 67 22:59:49.1	13 Aug. 67 11:05:45.96.		
Eccentricity	0.043696	0.043754	0.049471	0.0492825	0.33383	0.333538	0.338188	0.518333	0.276820		
Inclination, <sup>d</sup> deg	20.91	20.95	21.01	20.975	12.119	12.01	11.875	85.4	85.4		
Semimajor axis, km	1967.8	1967.93	1968.31	1967.619	2669.39	2669.80	2689.64	3753.148	2536.123		
Longitude of pericenter passage, <sup>e</sup> deg	57.8	55.8	332.9	331.1	2.0	354.7	342.4	10.9	15.3		
Latitude of pericenter passage, <sup>e</sup> deg	-2.0	-2.0	-4.0	-3.95	-1.06	-1.166	2.54	-5.2	1.6		
Period, min	130.55	130.56	130.54	130.54	206.41	206.38	208.62	344.0	191.1		

<sup>a</sup>III-E, 1b; 2d; and 4b follow, respectively, by one orbit. <sup>c</sup>Selenographic at epoch. <sup>e</sup>Selenographic at pericenter.

<sup>b</sup>Selenocentric, earth equatorial. Ref. 2. <sup>d</sup>To lunar equator.

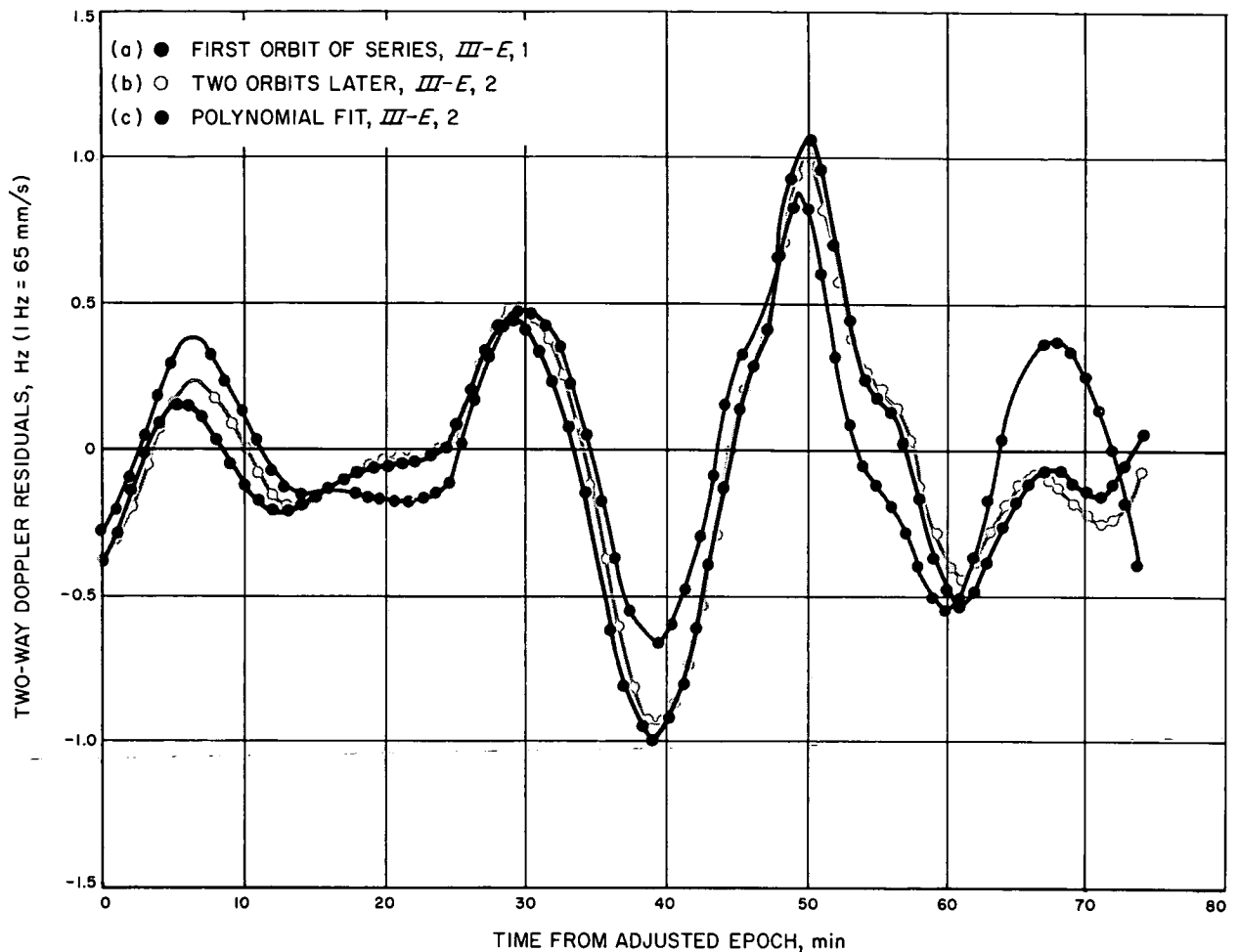


Fig. 7. Comparison of ODP and polynomial fits to two distinct orbits of Lunar Orbiter III-E, 1

Figure 2 (SPODP) is data from the same spacecraft some 5 days later. The change in residuals from Fig. 7 indicates that they do differ over longer time spans.

Figure 6 shows polynomial fits to four consecutive orbits of the same spacecraft (*Lunar Orbiter III-E*, orbit series 1 and 2, the same orbit set used in Fig. 7) by coded lines. The agreement between the polynomial and SPODP fits is shown in Fig. 7 for orbit 2C of *Lunar Orbiter III-E*. Since polynomial fits to the data were from a single station, it was possible to obtain residuals for all four orbits. (SPODP usually requires either two stations viewing, or adequate *a priori* on the spacecraft state vector to converge.)

The agreement between the four residual sets demonstrates both the quality of the polynomial fits to the raw data and the invariance of the residuals. In Fig. 6, orbit 2d

is degraded because of the missing data; polynomial fits are more sensitive to missing data than are the SPODP fits.

Figure 8 combines the tests illustrated in Figs. 6 and 7 and applies them to a new trajectory. *Lunar Orbiter III-E*, 3 covers data approximately 5 days after that acquired during the above orbits. Coded lines in Fig. 8 show: (1) the fit to the first of three sequential orbits by use of SPODP; the polynomial fit to the same data for comparison between the models; and fits to the two orbits following orbit 2C; again, the invariance of residuals for sequential orbits is illustrated. However, the residuals have changed dramatically in the 5 days time between that represented in Figs. 6 and 8.

The case of two different spacecraft flying similar trajectories, weeks apart, is illustrated in Fig. 9 with two high-eccentricity polar-orbiting spacecraft, *Lunar Orbiters IV-C* and *V-C*, respectively. As shown in



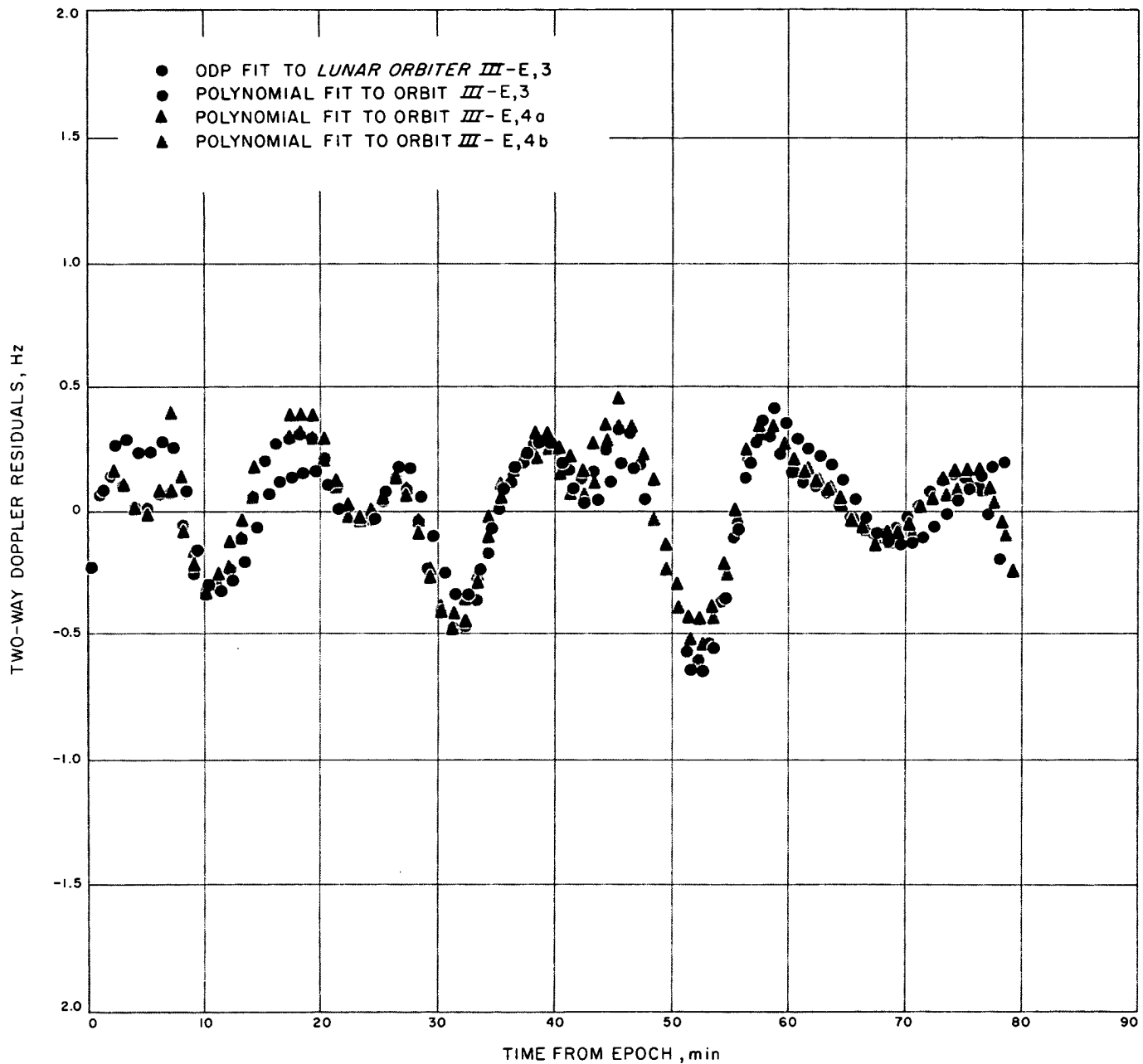


Fig. 8. Polynomial fits to three distinct orbits of Lunar Orbiter III-E, 3 and 4 with one ODP fit for comparison

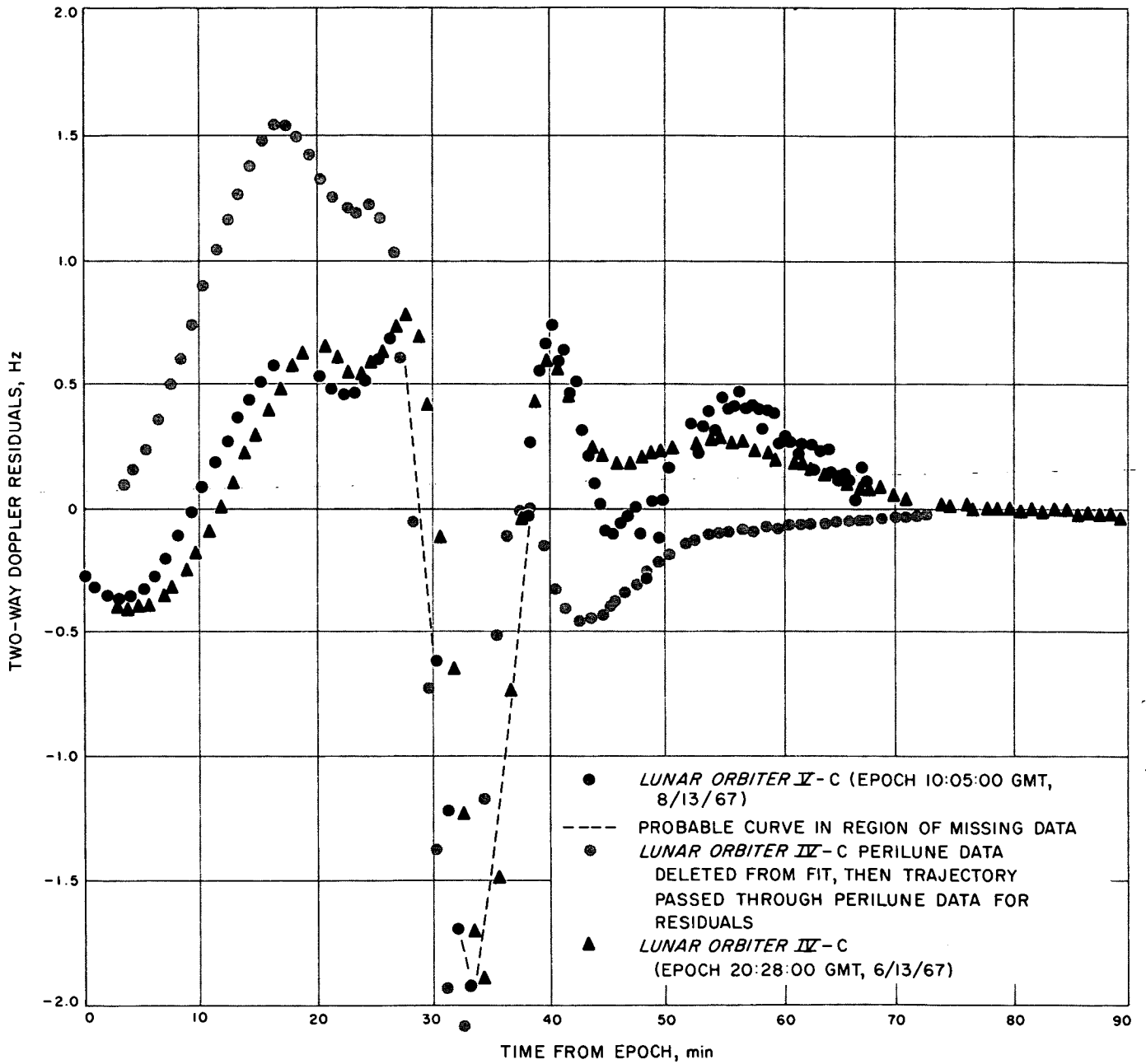


Fig. 9. Comparison of ODP fits to two distinct spacecraft (Lunar Orbiters IV-C and V-C) with similar trajectories

Table 2, the orbital parameters—most notably, the eccentricity—differ substantially. The lunar track, however, is similar (as can be seen from Fig. 1) and that fact manifests itself in the agreement between residuals. The very large plunge in the residuals constitutes the most spectacular such example observed in the study.

Figure 9 shows SPODP fits to orbits of *Lunar Orbiters IV-C* and *V-C*. Both the small inflection points and the very large variation agree in time and amplitude. The second line in the figure for *IV-C* was obtained by deleting the perilune data from a fit and iterating to a converged spacecraft state. This state was then integrated forward and passed through the perilune data without iteration. While the signature is obviously skewed and biased, the agreeable comparison of this with the same data span of the *IV-C* full orbit stands as additional evidence that the residuals we see are actually in the data.

There was some success in matching the largest residual signatures with such visible features on the moon as maria and rough highlands. These large residual variations appear, therefore, to correlate with the largest lunar elevation changes. This is not to say that all residuals correlate in this manner; in fact, the authors failed to find consistent correlations between the more typical residual signatures and elevations as reported on the lunar maps.

In the next section of the paper, additional comparisons are given that illustrate both the dependence of residuals on the lunar track and limitations of the SPODP and polynomial methods of fitting the data.

## V. Additional Cases and Evaluation of the SPODP and Polynomial Models

The key requirement of limiting SPODP to single-orbit fits has already been discussed, along with the tests that determined that this limitation resulted in the desired consistency of residuals after the fit. Figure 10 illustrates the independence of 1-orbit SPODP fits to change of epoch and length of data arc. Figure 11 gives a similar illustration for the polynomial model.

Figure 11 shows: (1) a polynomial fit to *III-E*, 2c by use of coefficients<sup>5</sup> 0, 2, 4 or 3, 0, 4—which are indistinguishable; and (2) a fit to the same data span but with the

<sup>5</sup>See Appendix A for a discussion of the polynomial program method and Appendix B for explanation of nomenclature used in describing the coefficients included in the fit.

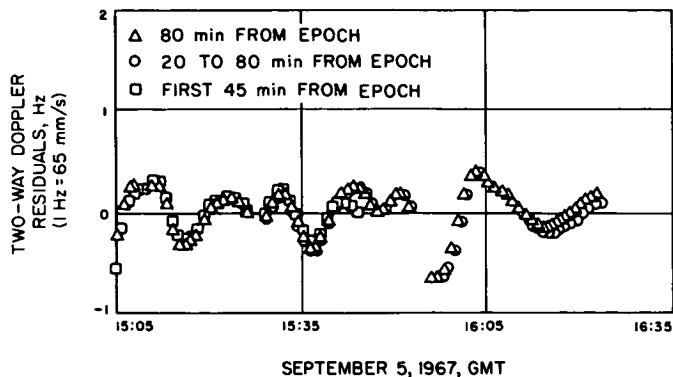


Fig. 10. ODP fits to one orbit of *Lunar Orbiter III-E*, 3 with distinct epoch and fit lengths

set 2, 0, 6 to illustrate the small changes that result from a slightly different set of coefficients. It will be shown below that the relative independence of the polynomial fit and the coefficient set solved for holds well for fits to the low-eccentricity trajectories only, such as in Fig. 11. It will be seen that the high-eccentricity orbits are more sensitive to the choice of coefficients in the polynomial model.

The third data trace in Fig. 11 is a fit to the same data with the epoch moved forward 20 min, which simultaneously reduces the arc length and alters the epoch. The consistency of fit is excellent, especially considering the fact that polynomial fitting schemes are usually extremely sensitive to both epoch and length of fit.

It is concluded that, under the stated limitations on arc length and low eccentricity, both SPODP and polynomial methods give consistent and stable residuals after the fit.

Both SPODP and polynomial fits are degraded somewhat for arcs with high eccentricity. The examples of *Lunar Orbiter III-E* trajectories used in the text all have low eccentricity ( $e = 0.04$ ). The more typical photo mission profiles have  $e = 0.3$  and 40 to 100-km perilunes.

The aforementioned *Lunar Orbiter III-E* trajectories have an advantage for the residual analysis used in this paper, in that their perilune is 150 km, and apolune is 300 km. This means that the spacecraft is always close enough to the lunar surface to be affected more or less uniformly by the local gravitational anomalies.

The higher-eccentricity orbits are within 500 km (an approximate cutoff point for the effects we desire) of the lunar surface for only one-third of the orbit. Furthermore,

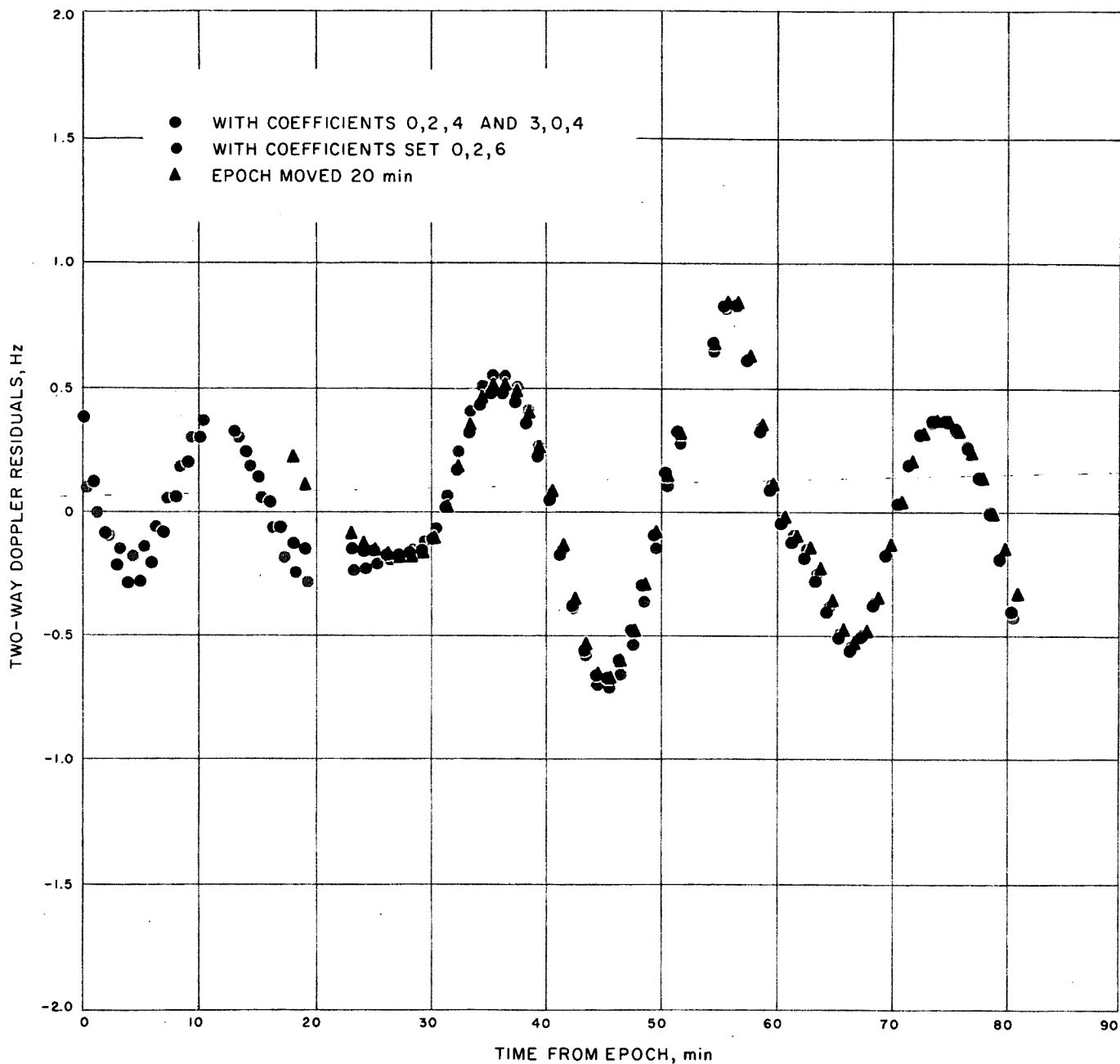


Fig. 11. Polynomial fits to one orbit of *Lunar Orbiter III-E, 2* with distinct epochs and coefficient sets

these trajectories are more difficult to fit with the desired consistency.

Figure 12 compares three fits to the same orbit of *Lunar Orbiter I-B, 3* data. The first plot is a fit to one full orbit with SPODP. The residuals for only the central portion of the orbit are shown, the 40-min period centered approximately at perilune. (Although the full orbit was fit, only the central 40-min data were plotted.)

The second plot was obtained by fitting only the 40 min data span shown with SPODP. The lack of consistency between the longer and shorter arcs, as fit with the same model (SPODP), is at variance with the agreement obtained when this test was applied to the low-eccentricity trajectories. It may not be too surprising in one sense; the high eccentricity orbits have longer period and span a larger fraction of the 360-degree circle between occultations than the low-eccentricity trajectories. (Occultation-to-occultation spans are 90 min for low eccentricity, 180 min for high eccentricity.)

Examination of the two SPODP curves in Fig. 12 reveals that a long-period factor of some kind has entered the residuals, since the left portion of the full fit is below the references, and the right portion is above it. The tendency to large, long-period residual signatures on the fits to longer arcs is already evident in this case; that it becomes dominant on 2- or 3-orbit fits can be seen in Ref. 1.

The third curve on Fig. 12 was derived by plotting the central 40 min of a polynomial fit to the same *full orbit* of data. The SPODP fit to the central 40 min of this pass agrees with the comparable portion of the polynomial fit to the whole orbit. The conclusion is clear; SPODP may begin to depart from true minimum residuals in less than one orbit. The basic conclusion remains, however, SPODP and polynomial fits agree and yield minimized residuals, providing the fit interval is not excessive. An estimate of 90 min for the data span would seem to be safe for production of true, minimum residuals in the sense brought out in footnote 4.

The polynomial program also suffers from exposure to higher-eccentricity data. Figure 13 shows: (1) a plot of *Lunar Orbiter I-B, 3*, residuals from a polynomial fit to the entire orbit by use of polynomial coefficients 2, 4, 6; (2) results of a polynomial fit to the central 80 min of these data by use of coefficients 3, 0, 6 (the set chosen out of a large sample precisely because it gave the best agreement); and (3) the results if the same polynomial set 2, 4, 6 is used for the 80 min as was employed in the full orbit fit. The reduction in amplitudes is understandable, even if unfortunate. As the data span is shortened, the third-order moon terms in the model tend to fit out the larger residual bumps caused by the local gravity. The conclusion is that the polynomial method will fit many high-eccentricity data spans quite well, but it is somewhat sensitive to the choice of coefficients if the gravity effects are to be accurately determined.

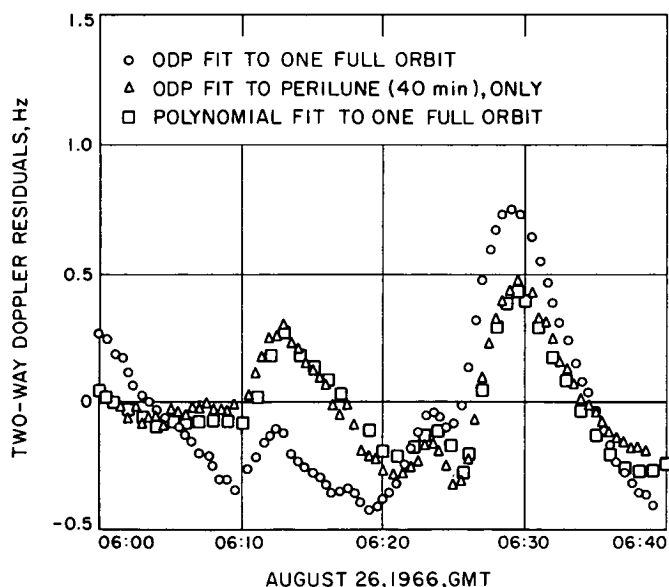


Fig. 12. Comparison of residuals from *Lunar Orbiter I-B, 3* in region of pericenter passage as determined by three distinct methods of computation

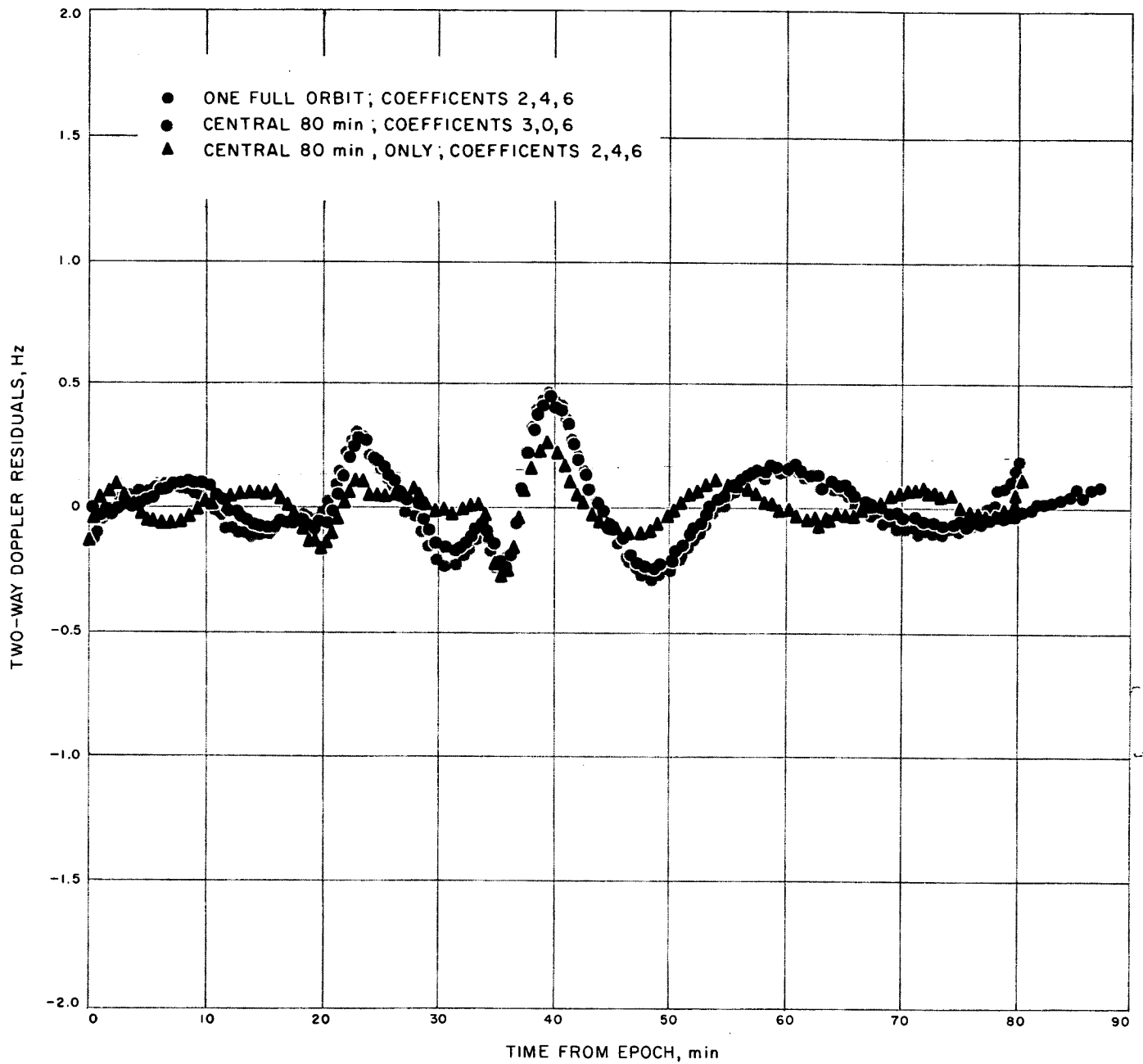


Fig. 13. Polynomial fits to one orbit of Lunar Orbiter I-B, 3 and to central 80 min, only, with two coefficient sets

We can now return to the question of comparing high-eccentricity spacecraft trajectories with similar lunar tracks. The polar orbiting *Lunar Orbiters IV-C* and *V-C*, already cited, are high-eccentricity examples. It so happened that SPODP fits seemed to agree well, while the polynomial program would not fit them at all. The tentative assumption was that SPODP produced signatures close to the true minimum and could stand alone. It is unlikely that the small and large inflections could agree

so well between two spacecraft unless the fits were correct; a spurious model-induced signature would almost certainly differ markedly.

Such was illustrated by the comparison of the curves of Fig. 14. These illustrate SPODP fits to *full orbits* of *Lunar Orbiters II-B, I-B, 1* and *I-B, 3*, respectively. We have seen that SPODP can yield skewed fits to full-orbit data spans of this kind. Both this fact and the agreement

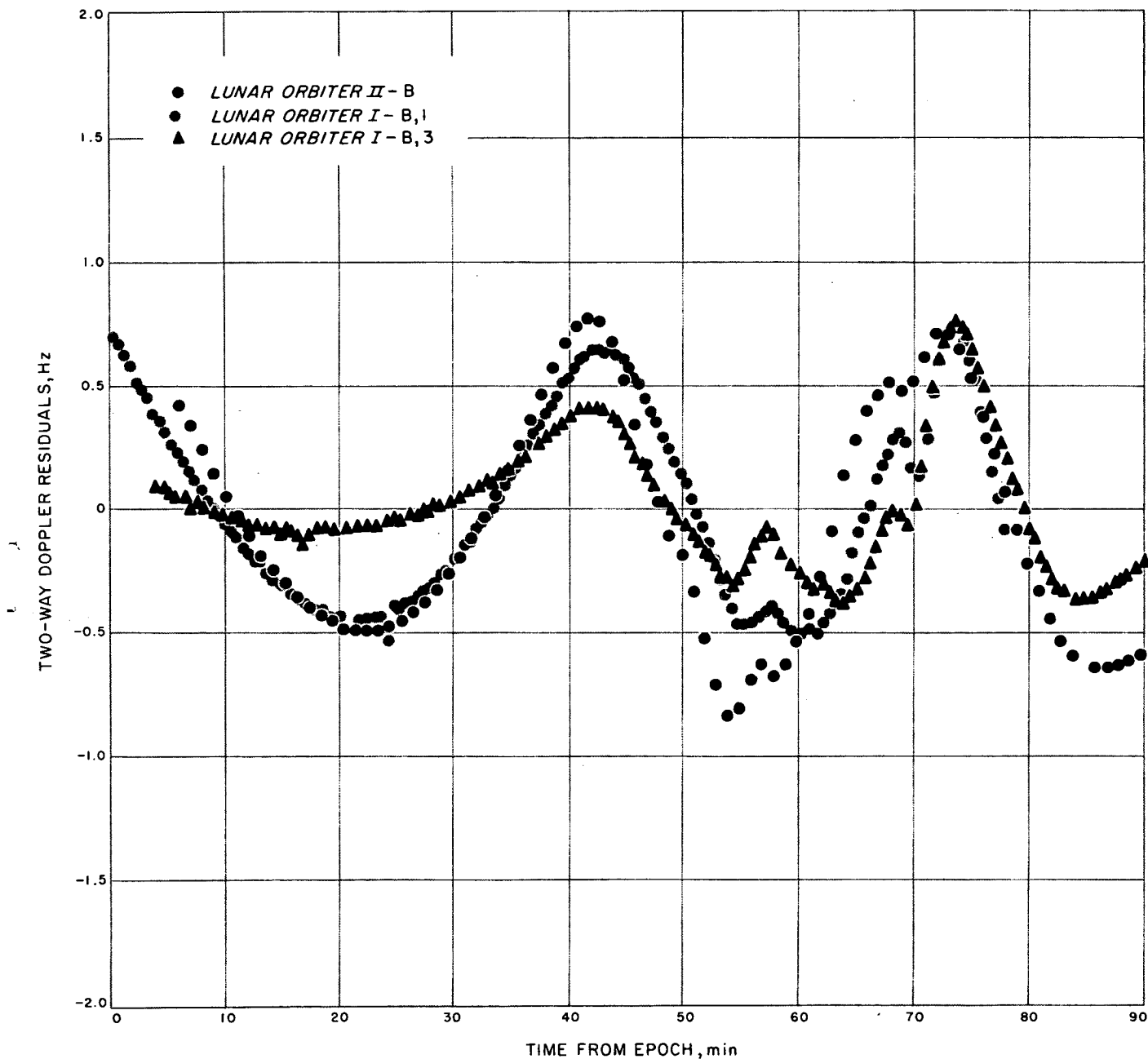


Fig. 14. ODP fits to two distinct spacecraft in three orbits, *Lunar Orbiters I-B, 1; I-B, 3; and II-B*

between residuals and the trajectory are illustrated. Particularly evident is the fact that the *Lunar Orbiter II-B* and *I-B, 3*, residual signatures contain similar *small* inflections at the same relative times. This permits us to identify the agreement between the residuals through the noise induced by the fitting procedure. The large-scale, long-period variations visible in the plots probably are not due to the local gravity but, rather, are introduced by the SPODP. The fact that they agree in a rough sense merely demonstrates that the same model will tend to make

similar errors when fitting similar trajectories. Note that the *Lunar Orbiter I-B, 1* and *I-B, 3* results (for the same spacecraft two orbits apart), do not agree any better than the *Lunar Orbiter II-B* vs the *I-B*—which fact indicates the relatively poorer quality of these fits than the low-eccentricity results given above.

Figure 15 illustrates the same trajectories as Fig. 14, with a polynomial model. All three data spans were fit with the same polynomial model, namely,  $A = 2, E = 4$ ,

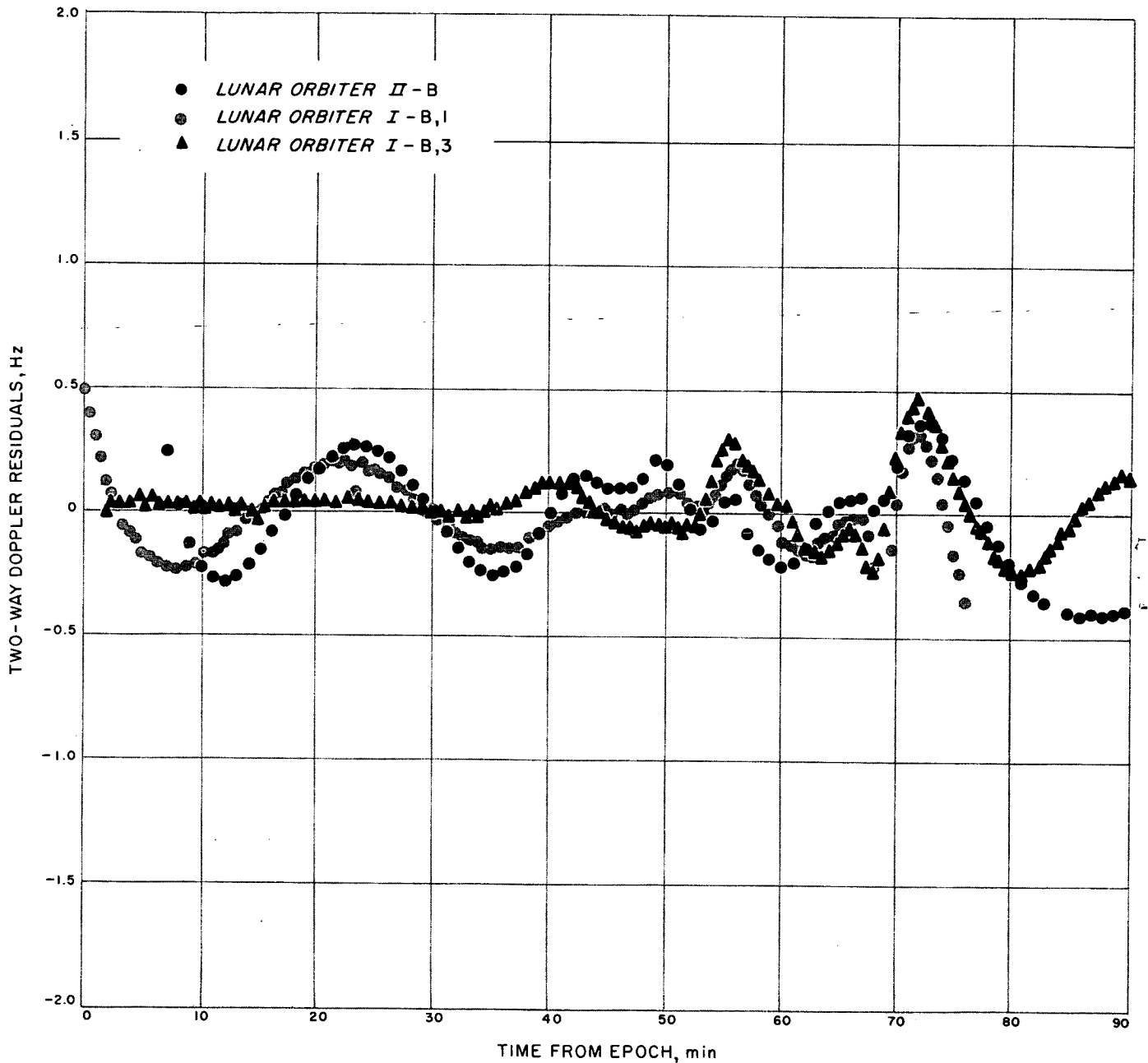


Fig. 15. Polynomial fits to two distinct spacecraft orbits, *Lunar Orbiters I-B* and *II-B*



$M=6$ . There is some difficulty making a neat polynomial fit without eliminating the desired residuals; it is, relatively speaking, a poorer filter than when applied to low-eccentricity data. As with SPODP, the small- and medium-sized signatures correlate fairly well, with a tendency for at least two of the fits to introduce longer-period, spurious variations clearly visible. The *Lunar Orbiter I-B, 3*, curve is probably the best indication of the true minimized residuals. They are *zero* on both ends of the trajectory, with the near-perilune portion of the trajectory revealing the typical 0.5-Hz signatures (only the middle half of the full orbits are actually plotted). It is expected that the SPODP will yield results closely related to those of Fig. 15 when fitting the *I-B, 3* trajectory if and when it can be improved for the longer data spans. The polynomial fit was not perfect, but it does give a reliable set of residuals for certain trajectories, which may be compared with whatever improved models may emerge after further study.

Because the SPODP will consistently fit only a single orbit of data, one might naturally ask why the model has failed. Since any model is bound to be incomplete, the departures from reality that exist will map into a complex array of errors in the fit. We engineers tend to make the dangerous assumption that they all tend to cancel out, anyway.

Some will argue that using SPODP, which lacks cognizance of the high-frequency gravitational anomalies discussed in this paper, may still permit a solution for the longer-period gravitational effects. To an extent, this is no doubt true; but results in Fig. 3 raise some doubt in the authors' minds.

Figure 3 was obtained by first integrating a trajectory with point-mass moon and computing doppler, then differencing the doppler derived from integrating the moon with mass points placed uniformly along the lunar surface directly below the spacecraft. The mass points alternate sign and sum to *zero*. There was no fit to the data, only the straight integrations and differencing.

Whereas a sinusoidal variation of high frequency, centered on *zero*, was expected, actual results were those in Fig. 3. Since the curve crosses *zero* at the start of each subsequent orbit (within the 0.5-Hz amplitude of a single perturbation), and does so for each of the several cases run, the error is not being caused by faulty integration but, rather, arises from the fact that the perturbative accelerations do not sum to *zero* until the end of a full orbit. Implicit in this is the danger that a model which

fails to account for the small, high-frequency variations would attempt to fit out the long, one-cycle per spacecraft orbit residuals, of ever increasing amplitude, which result from differencing the real data and that computed by an *incomplete* trajectory model.

Neither Fig. 3, alone, nor its repeatable example, is claimed, necessarily, to show that SPODP suffers from this specific symptom. *It is felt, however, that by using the fits to longer arcs with SPODP (accepting the increased residuals), solutions may be generated that primarily represent unidentified model-induced errors, rather than the desired long-period variations in the spacecraft motion.*

To summarize in another way, it would seem advisable to first improve the short arc (from one to several orbits) model before relying on these fits for long-arc analysis.

## VI. Possible Direction of Future Work

With the assumption that the doppler residuals from each orbit of a *Lunar Orbiter* spacecraft are a direct measure of the local gravity field, the immediate plan is to estimate some small set of mass points along the trajectory of a single orbit. If this plan is successful, then the reduction of a few sequential orbits simultaneously will be attempted. As a mass-grid is built from these solutions, consistency (or lack thereof) can be demonstrated.

If consistent and successful, these solutions either could be reduced statically to a high-order harmonic set (as proposed by Jack Lorell of JPL), or could be analyzed for simplification and possible correlation with selenological history, etc. It is possible that mapping of the residual-derivative (accelerations) to the lunar surface would serve to solve the lunar surface and gravity field for the frontside directly, without recourse to the more complex fitting scheme. Either way, it may well turn out that *Lunar Orbiter* was an admirable flying gravimeter.

The problem of defining the moon's backside remains, since there are no data available to solve it directly. All proposed indirect methods of solution appear to fall back on measuring the variation in orbital parameters or spacecraft coordinates over many orbits. To fit arcs of from two to several orbits, it may be possible to solve for the effect of the backside by considering its total effect to be a solve-for, instantaneous spacecraft maneuver. This might permit an improved fit to more than a single orbit, but will only solve out the backside for the single arc in question.

The *Apollo* project is concerned about the accuracy of short-arc fit-prediction capabilities. A considerable effort will be made to attain improvement of a magnitude or better in this area, which appears to be the real strength of the short-arc point mass approach.

## VII. Summary

To obtain consistent residuals, the SPODP must be run with data arcs of one orbit and with minimal (triaxial or spherical) harmonic coefficients. With that approach, the residuals from one spacecraft correlate with those from another if they fly the same, or similar, lunar track. This

correlation ties the residuals to the local-lunar gravitational field.

The frequencies observed in the residuals are too high to be included effectively in a harmonic expansion of the lunar potential unless the order of the latter can be increased substantially over current standards. This fact further suggests the need for a different lunar potential model and approach to the problem if improvement in the fit and prediction is to be achieved. It is possible that such a model would best be derived directly either from analysis of the residuals or by solving for a mass point grid near the lunar surface.

## Appendix A<sup>6</sup>

### The Polynomial Fitting Program and Method

Raw doppler data may be considered to be composed of three components: one, the motion of the observer, another due to the conic motion of the orbiter and the lower harmonics of the moon's potential, and finally, the higher harmonics of the moon's potential. The filter removes the first two components and leaves the higher harmonics.

This operation is accomplished by first estimating the motion of the observer and the conic motion, then generating residuals  $r$ , where

$$r = \Delta\rho - \Delta\rho_e$$

and where  $\Delta\rho$  is the observed data (two-way doppler), and  $\Delta\rho_e$  is the estimated motion, which is given by

$$\Delta\rho_e = \int_{t_1}^{t_2} \dot{\rho}_e dt$$

where  $(t_2 - t_1)$  is the doppler count time.

<sup>6</sup>This text was supplied by S. McReynolds and P. Dyer as description of their polynomial fitting scheme.

The expansion for  $\dot{\rho}_e$  was chosen to be

$$\dot{\rho}_e = C_0 + C_1 t + C_2 t^2 + \sum_{i=1}^N (a_i \cos if + b_i \sin if)$$

where  $t$  is the time and  $f$  is the true anomaly. The algebraic terms represent primarily the motion of the observer, while the remaining terms represent the conic motion of the orbiter, as well as the lower harmonics of the moon's potential.

This expansion was chosen because the coefficients  $a_i$  and  $b_i$  converge rapidly. The terms  $a_1 \cos f$  and  $b_1 \sin f$  fit the contribution from conic motion of the orbiter, and the other harmonic terms would be *zero* if the moon were at infinity. In practice, the remaining terms are *non-zero* because of parallax effects. The norm of  $a_2$  and  $b_2$  is approximately 1/300 of  $a_1$  and  $b_1$ . The ratio of the succeeding terms is approximately equal to the eccentricity.

The computational scheme to fit the data was based on a Householder transformation technique (Refs. A-1 and A-2) and was programmed by Richard Hanson.

## Appendix B

### Polynomial Model Coefficients Nomenclature

The polynomial program admits three classes of solve-for coefficients:

1. Ordinary  $n$ th order algebraic polynomials  
( $a_0 + a_1X + a_2X^2 + \dots$ )
2. Circular functions of the earth's rotation using sin and cos for 1st through  $n$ th harmonic, as desired.
3. Elliptical functions, sin and cos terms in true anomaly, for the spacecraft motion about the moon (again permitting 1st through  $n$ th harmonics, as required).

Such terms are designated by  $A$  for algebraic,  $E$  for earth and  $M$  for moon, respectively. They are also shown in the following form:  $A, E, M$  or  $3, 2, 4$  meaning, for instance,  $A = 3, E = 2, M = 4$ . This example would have a quadratic algebraic polynomial (three coefficients), a first-order earth term (sin and cos), and a second-order moon model. Note that the  $E$  and  $M$  orders are one-half the coefficient, since there are sine *and* cosine coefficients for each order.

The analytic definitions of these parameters are given in Appendix A.

### References

1. Lorell, J., and Sjogren, W. L., *Lunar Orbiter Data Analysis*, Technical Report 32-1220. Jet Propulsion Laboratory, Pasadena, Calif., Nov. 15, 1967.
  2. Warner, M. R., and Nead, M. W., *SPODP—Single Precision Orbit Determination Program*, Technical Memorandum 33-204. Jet Propulsion Laboratory, Pasadena, Calif., Feb. 15, 1965.
  3. *Transactions of Xth COSPAR Meeting, July 17–28, 1967, London* (to be published).
- A-1. Businger, P., and Golub, G., "Linear Least Squares Solutions by Householder Transformations," *Numerical Math. Vol. 7*, pp. 269–275, 1965.
- A-2. Hanson, R. J., and Lawson, C. L., *Extensions and Applications of the Householder Algorithm for Solving Linear Least-Squares Problems*, Jet Propulsion Laboratory, Pasadena, Calif. (to be published).